Establishing Corneal Cross-Linking With Riboflavin and UV-A in the Mouse Cornea In Vivo: Biomechanical Analysis

Arthur Hammer,[1] Sabine Kling,[1,2] Marc-Olivier Boldi,[3] Olivier Richoz,[1] David Tabibian,[1] J. Bradley Randleman,[4] and Farhad Hafezi[2,5,6]

[1]Laboratory for Ocular Cell Biology, University of Geneva, Geneva, Switzerland
[2]Center for Applied Biotechnology and Molecular Medicine (CABMM), University of Zurich, Zurich, Switzerland
[3]Research Center for Statistics, University of Geneva, Geneva, Switzerland
[4]Department of Ophthalmology, Emory University, Atlanta, Georgia, United States
[5]Department of Ophthalmology, University of Southern California, Los Angeles, California, United States
[6]ELZA Institute, Dietikon/Zurich, Switzerland

Correspondence: Arthur Hammer, Laboratory for Ocular Cell Biology, University of Geneva, Rue Michel Servet 1, 1206 Geneva, Switzerland; arthur.hammer6@gmail.com.

AH and SK contributed equally to the work presented here and should therefore be regarded as equivalent authors.

Submitted: June 5, 2015
Accepted: August 26, 2015

Citation: Hammer L, Kling S, Boldi M-O, et al. Establishing corneal cross-linking with riboflavin and UV-A in the mouse cornea in vivo: biomechanical analysis. *Invest Ophthalmol Vis Sci*. 2015;56:6581–6590. DOI:10.1167/iovs.15-17426

Purpose. To establish corneal cross-linking (CXL) with riboflavin and UV-A in in the mouse cornea in vivo and to develop tools to measure the biomechanical changes observed.

Methods. A total of 55 male C57BL/6 wild-type mice (aged 5 weeks) were divided into 14 groups. Standard CXL parameters were adapted to the anatomy of the mouse cornea, and riboflavin concentration (0.1%–0.5%) and fluence series (0.09–5.4 J/cm^2) were performed on the assumption of the endothelial damage thresholds. Untreated and riboflavin only corneas were used as controls. Animals were killed at 30 minutes and at 1 month after CXL. Corneas were harvested. Two-dimensional (2D) biomechanical testing was performed using a customized corneal holder in a commercially available stress-strain extensometer/indenter. Both elastic and viscoelastic analyses were performed. Statistical inference was performed using *t*-tests and specific mathematical models fitted to the experimental stress-strain and stress-relaxation data. Adjusted *P* values by the method of Benjamini and Hochberg are reported.

Results. For all CXL treatment groups, stress-relaxation showed significant differences ($P < 0.0001$) after 120 seconds of constant strain application, with cross-linked corneas maintaining a higher stress (441 ± 40 kPa) when compared with controls (337 ± 39 kPa). Stress-strain analysis confirmed these findings but was less sensitive to CXL-induced changes: at 0.5% of strain, cross-linked corneas remained at higher stress (778 ± 111 kPa) when compared with controls (659 ± 121 kPa).

Conclusions. Cross-linking was induced in the mouse cornea in vivo, and its biomechanical effect successfully measured. This could create opportunities to study molecular pathways of CXL in transgenic mice.

Keywords: corneal cross-linking, CXL, mouse cornea, corneal biomechanics, keratoconus

Corneal cross-linking with riboflavin and UV-A, initially introduced by Spoerl et al.,[1,2] is a method to increase corneal stiffness and to arrest corneal ectatic disorders like keratoconus and ectasia after refractive laser surgery[3] with a follow-up of several years.[4,5] The procedure is based on the combination of the photosensitizer riboflavin and UV-A irradiation and has initially been tested in ex vivo porcine corneas.[6] To analyze the potential phototoxic effect on the corneal endothelium at high UV doses and to adjust riboflavin concentration, CXL was subsequently tested in vivo on rabbit corneas.[7] A few years only after successful introduction of CXL into clinical ophthalmology,[8] the frequency of penetrating keratoplasties has been considerably reduced.[9]

Although already used extensively in clinical practice, CXL remains a relatively new technique needing further optimization. A number of new clinical treatment protocols have emerged in the past few years and have rapidly been used clinically without proper laboratory validation. Accelerated CXL is based on the Bunsen-Roscoe law, which states that the photochemical effect is proportional to the irradiance multiplied by the time of irradiation. This may mean that irradiation time could be shortened when using a higher UV irradiance. The efficacy of this treatment option, however, is unclear, and accelerated CXL may be less effective than CXL using the original protocol.[10] Corneal cross-linking is an oxygen-dependent process.[11] Pulsed CXL represents yet another new protocol that tries to overcome low oxygen saturation during irradiation at high UV-A light irradiances.[12] However, clinical and experimental evidence did not show significant differences between the pulsed and standard CXL protocol.[13–15]

These unsuccessful implementations show that there is a need for a better understanding of the cellular and molecular events occurring during CXL.

Most approaches to determine CXL efficacy focus on analysis of corneal biomechanics. There are only few and rather inaccurate approaches to determine the biomechanical efficacy of CXL in vivo; thus, clinicians have to rely on indirect signs like corneal topography and pachymetry maps. For ex vivo measurements, there are more accurate but destructive methods available to determine the actual biomechanical

Table 1. Adaptation of CXL Parameters to the Mouse Cornea

Name	Vit. B2, %	Irradiance, mW/cm²	Irradiation Time, min:s	Fluence, J/cm²	Time Between Treatment and Biomechanical Measurement	Stress-Strain, *n* eyes	Stress-Relaxation, *n* eyes
Virgin (control)	X	X	X	X	X	10	10
3 mW, 30 min, 1 mo	0.5	3	30	5.4	1 mo	9	9
9 mW, 10 min, 1 mo	0.5	9	10	5.4	1 mo	8	8
18 mW, 5 min, 1 mo	0.5	18	5	5.4	1 mo	9	9
9 mW, 2:50 min, 1 mo	0.27	9	02:50	1.53	1 mo	14	14
9 mW, 2 min, 1 mo	0.5	9	2	1.08	1 mo	6	6
0.5% ribo, 1 mo (control)	0.5	X	X	X	1 mo	8	8
0.27% ribo, 1 mo (control)	0.27	X	X	X	1 mo	8	8
9 mW, 10 min	0.5	9	10	5.4	30 min	5	5
0.5% ribo (control)	0.5	X	X	X	30 min	5	5

%, riboflavin concentration; X, not applicable; ribo, riboflavin.

properties of the corneal tissue. The golden standard technique consists of measuring the stress-strain curve and determining the Young's modulus.[1,2,6,11,12,16] Viscoelastic testing, including creep and relaxation tests,[17–19] has recently emerged as an option. However, a methodologic problem with ex vivo testing is that the tissue is subjected to hydration and other degrading processes soon after enucleation. These changes and the preservation media both modify the biomechanical properties[20] and affect accuracy of testing.

The main problem of optimizing CXL treatment parameters is that the underlying working principle of CXL can only be vaguely assumed: CXL might cross-link collagen fibers and/or proteoglycans, but could also affect gene expression. The latter is supposed, as keratoconus shows a genetic component.[21–24] A better understanding of the cellular and molecular events occurring during CXL might help in establishing optimized treatment modalities.

For this purpose, we established the biomechanical measurement after CXL in the mouse cornea in vivo, and tested whether the biomechanical effect can reliably be measured. The corneal cross-linking procedure in mice has been previously introduced.[25]

Methods

Specimens

All procedures concerning animals in this study adhered to the ARVO statement for the Care and Use of Animals in Vision Research. A total of 55 male C57/BL6 mice aged 5 weeks (Charles River Laboratories, Chatillon-sur-Chalaronne, France) were divided into two sets and treated with specific CXL parameters (Tables 1, 2).

In set 1 ($n = 41$ mice), CXL fluence and riboflavin (ribo) concentration parameters used in the human setting were applied and compared with settings that were adapted to the reduced thickness of the mouse cornea.

In set 2 ($n = 14$ mice), the fluence was consecutively reduced to determine the threshold level for effective CXL in the mouse cornea.

CXL Treatment Parameters

Since the mouse cornea is approximately five times thinner than the human cornea (100 μm[26] vs. 530 μm[27]) the CXL treatment parameters were adapted to prevent endothelial damage. For this purpose, we performed riboflavin concentration series (0.1%–0.5%), UV irradiance series (3–18 mW/cm²), and UV irradiation time series (30 seconds to 30 minutes; Tables 1, 2).

The Lambert-Beer law was used to ensure that in all cases the endothelium absorbed equal or less UV energy compared with standard CXL in humans:

$$T = \frac{I}{I_0} = e^{-\varepsilon \cdot th \cdot c} \quad (1)$$

where T is the transmittance, I_0 the intensity of the incident light, I the intensity at the endothelium, c the concentration of the riboflavin, th the thickness of the cornea, and ε the absorptivity of riboflavin.

Treatment Protocol

The mice were anesthetized with a mixture of ketamine 100 mg/kg (Ketalar; Pfizer AG, Zurich, Switzerland) and xylazine 10 mg/kg (Rompun; Bayer AG, Leverkusen, Germany), administered subcutaneously. Corneas were soaked with tetracaine 1% SDU Faure (Novartis Pharma Schweiz AG, Risch, Switzerland) for 2 minutes, and 35% alcohol for 2 additional minutes. The epithelium was removed using an ophthalmologic surgical sponge (Sugi-Saugkeil, 17 × 8 mm; Dosch, Medizintechnik, Heidelberg, Germany). Riboflavin (vitamin B2; Streuli Pharma AG, Uznach, Switzerland) was diluted to the desired concentration using PBS (Dulbecco's PBS; Sigma-Aldrich GmbH,

Table 2. Determining the Threshold Fluence for Effective CXL in the Mouse

Name	Irradiance, mW/cm²	Irradiation Time, min	Fluence, J/cm²	Stress-Strain, *n* eyes	Stress-Relaxation, *n* eyes
3 mW, 3 min	3	3	0.54	4	4
3 mW, 1 min	3	1	0.18	9	6
3 mW, 30 s	3	0.5	0.090	4	4
0.1% ribo (control)	X	X	X	5	4

The riboflavin concentration was 0.1% and the time between treatment and biomechanical analysis was 30 minutes for all groups.

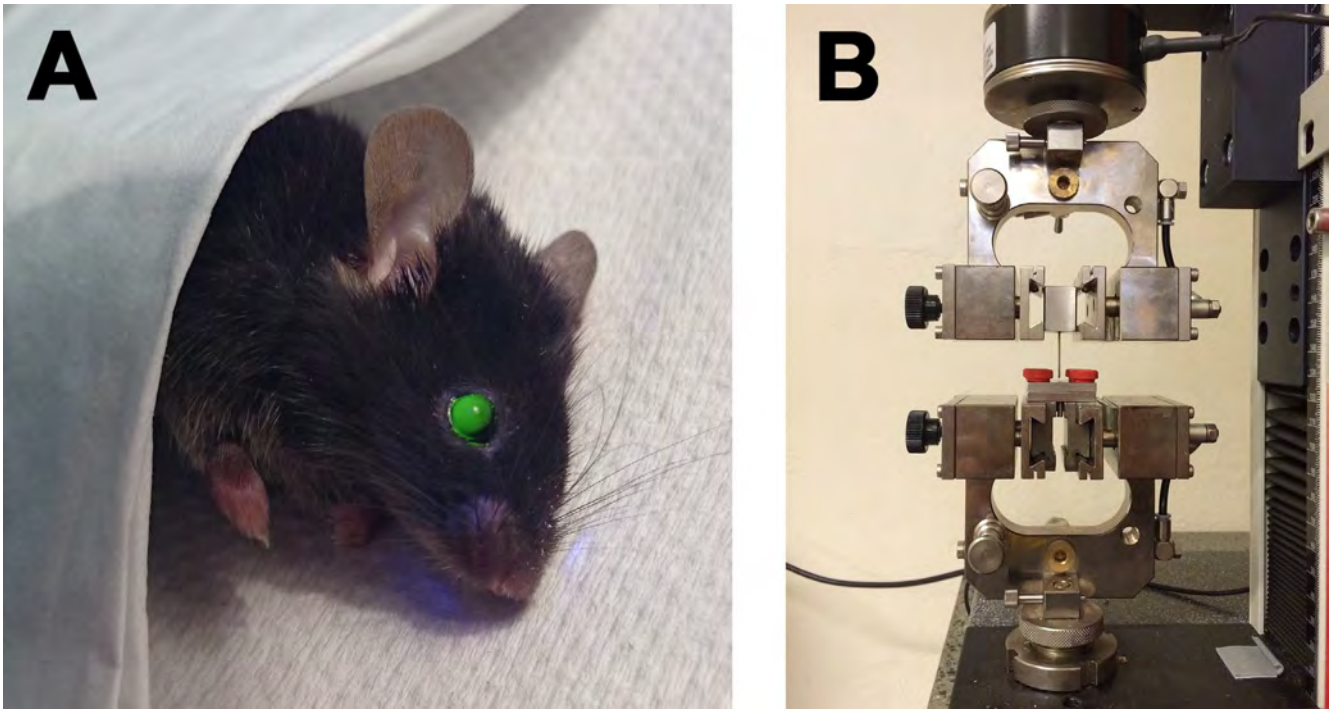

FIGURE 1. (A) Mouse undergoing CXL treatment, showing riboflavin fluorescence of the cornea. (B) Experimental setup: corneal holder mounted on the extensometer/indenter.

Steinheim, Germany), and the photosensitizing solution applied on the de-epithelialized cornea for 20 minutes. The corneal cross-linking treatment was performed according to Table 1. After UV-A irradiation, ofloxacin ointment (Floxal; Bausch and Lomb Swiss AG, Zug, Switzerland) was applied.

Customized Stress-Strain Extensometry

Due to the small size of the mouse eye, a custom holder was developed to fixate the mouse cornea circumferentially for biomechanical measurements (Fig. 1). The holder was made of steel with a small central hole of 1.6 mm. The cornea was then placed into the lower part over the central hole, and the upper part mounted by means of screws to fix the cornea. Circular indentations were milled into the surrounding of the central hole to prevent slippage. The holder was then mounted on the stress-strain extensometer/indenter (Z0.5; Zwick GmbH & Co., Ulm, Germany). A custom metal indenter with spherical surface (0.5-mm radius) was used to apply a three-dimensional force on the corneal surface through the central hole of the holder. The system was operated in compression mode with the corresponding software (testXpert II; Zwick GmbH & Co.).

Biomechanical Analysis

For biomechanical analysis, mice were euthanized, eyes were enucleated, and the corneas excised circumferentially near the limbus, leaving a small scleral rim. Corneas were then fixed within the holder, and a drop of PBS was applied on top of the central hole to prevent dehydration during testing.

The biomechanical analysis consisted of three steps: (1) preconditioning with three repetitions of stress-strain cycling between 0.05 and 0.4 N; (2) stress-relaxation testing during 120 seconds under the application of an initial force of 0.4 N, corresponding to a stress of 663 kPa; and (3) stress-strain extensometry with increasing force until specimen break. For stress relaxation testing, a constant strain was applied on the cornea and the decrease in stress recorded. For stress-strain testing, the indenter was moved downward at a constant speed, which applied an increasing force on the cornea and the corresponding stress measured.

In this context, stress can be calculated by:

$$\sigma = \frac{F}{2 \cdot \pi \cdot R \cdot th} \quad (2)$$

where σ is stress, F is the applied force, R is the radius of the central hole in the corneal holder, and th is the corneal thickness. Within the maximal vertical indentation observed (Δ_{max}), we can assume that the force applied by the indenter is orthogonal to the corneal surface and hence induces tensile stress as shown in Figure 2.

Strain can be calculated by:

$$\varepsilon = \frac{\Delta^2 + R^2}{2\Delta R} \cdot sin^{-1}\left(\frac{2\Delta R}{\Delta^2 + R^2}\right) - 1 \quad (3)$$

where ε is strain and Δ is the vertical indentation measured.

Appendix 1 provides more details about the derivation of Equations 2 and 3.

Comparisons

Out of the different combinations of conditions, biomechanical tests, and postop times, we did four major comparisons: (1) stress-strain versus stress-relaxation analysis to determine if one technique is superior to the other, (2) different fluences to identify the lowest threshold for CXL, (3) immediate effect of CXL versus 1 month after to study if there are differences between short- and long-term, and (4) different irradiances at the same fluence to verify the validity of the Bunsen-Roscoe law.

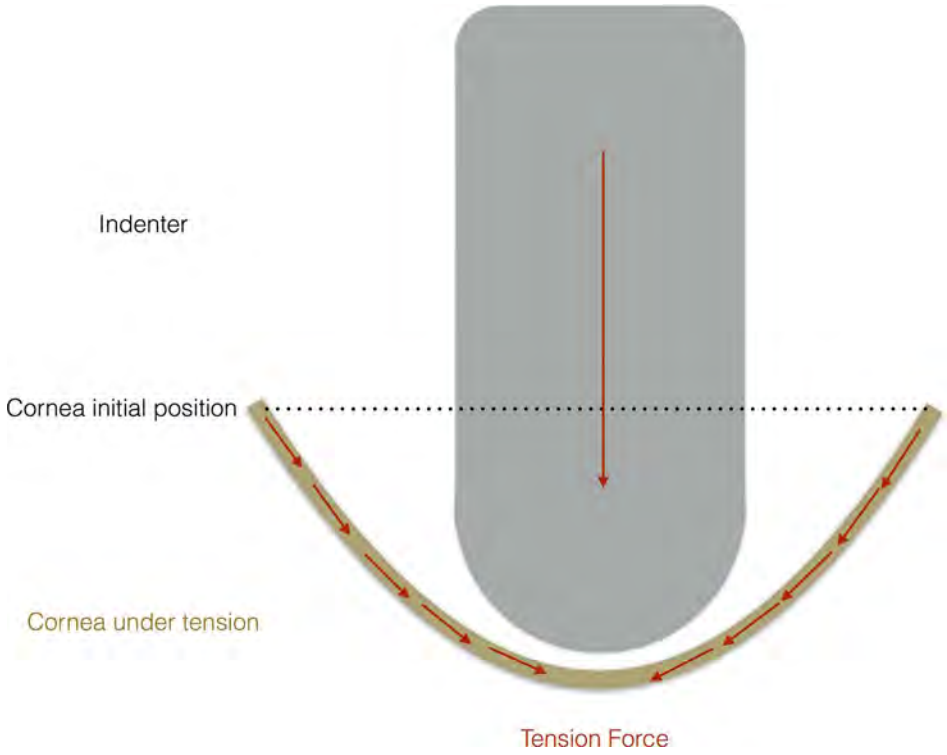

FIGURE 2. Scheme of the experimental setup describing the applied tensile force onto the corneal surface using a customized indenter.

Statistical Analysis

Student's *t*-test (XLSTAT, version 2014.6.01; Addinsoft, Paris, France) was performed to compare the overall difference between CXL treatment and control groups: in the stress-strain analysis at 0.5% strain and in the stress-relaxation analysis at 120 seconds.

The statistical analysis was further refined taking into account all points along the curves of the stress-strain and stress-relaxation measurements. For this purpose, the Research Center for Statistics at the University of Geneva used specific mathematical models that were fitted to the experimental stress-strain and stress-relaxation data. Unlike the Student's *t*-test or ANOVA, the approach of fitting a mathematical model to the experimental data allowed us to compare the entire curves additionally to individual points only.

The Prony series is a physical model describing the stress-relaxation curves in a range between 0 and 119 seconds:

$$F(t) \sim \sigma(t) = \sigma_\infty + \sigma_1 \cdot e^{-\frac{t}{\tau_1}} + \sigma_2 \cdot e^{-\frac{t}{\tau_2}} \qquad (4)$$

where $F(t)$ is the force at time t, $\sigma(t)$ is the stress at time t, σ_∞ is the asymptotic stress, σ_1 and σ_2 are the short-term stress and τ_1 and τ_2 are the corresponding relaxation times. The Prony series are typically expressed in terms of moduli, which is the case if Equation 4 is divided by the constant strain ε_{const} that was applied during the measurement.

For the statistical analysis, this basic physical model (Equation 4) was translated into a nonlinear mixed model.[28] Like the repeated measure ANOVA, it extends the ANOVA taking into account for the correlations between repeated observations from the same subject. Nonlinear models generalize models in the same way.

$$\begin{aligned} &F_{ijt} = F_{\infty ij} + F_{1ij} e^{-\frac{t}{\tau_{1ij}}} + F_{2ij} e^{-\frac{t}{\tau_{2ij}}} + \delta_{ijt}, \delta_{ijt} \sim N(0, \lambda^2) \\ &F_{\infty ij} \sim N(F_\infty, \lambda_\infty^2), F_{1ij} \sim N(F_1, \lambda_1^2), F_{2ij} \sim N(F_2, \lambda_2^2) \\ &\tau_{\infty ij} \sim N(\tau_\infty, \gamma_\infty^2), \tau_{1ij} \sim N(\tau_1, \gamma_1^2), \tau_{2ij} \sim N(\tau_2, \gamma_2^2) \end{aligned} \qquad (5)$$

The index i is for the subject and j is for the treatment. All the random components are assumed independent and normally distributed (notation $\sim N$). In Equation 5, λ is the within-subject standard deviation, and λ_∞, λ_1, λ_2, γ_∞, γ_1, γ_2 are the between-subject standard deviations for each model parameter. The model is fitted to the observed stress series using a statistical computer program (package nlme v3.1-111 of

TABLE 3. Significant Differences in Stress-Strain and Stress-Relaxation Tests Between CXL and Control Groups

Groups Compared		Stress-Strain *P* Value	Stress-Relaxation *P* Value
0.5% ribo, 1 mo (control)	0.5% ribo (control)	0.0027	<0.0001
18 mW, 5 min, 1 mo	0.27% ribo, 1 mo (control)	0.0276	<0.0001
9 mW, 2 min, 1 mo	Virgin (control)	0.0043	<0.0001
9 mW, 2:50 min, 1 mo	Virgin (control)	0.0219	<0.0001
3 mW, 30 min, 1 mo	Virgin (control)	0.0219	<0.0001
18 mW, 5 min, 1 mo	Virgin (control)	0.0016	<0.0001
9 mW, 10 min, 1 mo	Virgin (control)	0.0043	<0.0001

Table 4. Higher Sensitivity of Stress-Relaxation Test Compared With Stress-Strain Test

Groups Compared		Stress-Strain *P* Value	Stress-Relaxation, *P* Value
Virgin (control)	0.5% ribo (control)	0.0509	<0.0001
9 mW, 2:50 min, 1 mo	0.5% ribo, 1 mo (control)	0.7393	<0.0001
9 mW, 2 min, 1 mo	0.5% ribo, 1 mo (control)	0.6844	<0.0001
3 mW, 30 min, 1 mo	0.5% ribo, 1 mo (control)	0.7393	<0.0001
18 mW, 5 min, 1 mo	0.5% ribo, 1 mo (control)	0.1935	<0.0001
9 mW, 10 min, 1 mo	0.5% ribo, 1 mo (control)	0.5407	<0.0001
9 mW, 2:50 min, 1 mo	0.27% ribo, 1 mo (control)	0.5407	<0.0001
9 mW, 2 min, 1 mo	0.27% ribo, 1 mo (control)	0.1094	<0.0001
9 mW, 10 min, 1 mo	0.27% ribo, 1 mo (control)	0.1373	<0.0001
3 mW, 30 min, 1 mo	0.27% ribo, 1 mo (control)	0.5407	<0.0001
9 mW, 2 min, 1 mo	9 mW, 2:50 min, 1 mo	0.4578	0.0064
3 mW, 30 min, 1 mo	9 mW, 2 min, 1 mo	0.4578	0.0160
9 mW, 10 min, 1 mo	9 mW, 2 min, 1 mo	0.7392	<0.0001
9 mW, 10 min	0.5% ribo (control)	0.7944	<0.0001
3 mW, 3 min	0.1% ribo (control)	0.7696	<0.0001
3 mW, 1 min	0.1% ribo (control)	0.1701	<0.0001
3 mW, 30 s	0.1% ribo (control)	0.1712	<0.0001
3 mW, 30 s	3 mW, 1 min	0.8152	0.0056
3 mW, 30 s	3 mW, 3 min	0.3086	0.0002

Table 5. No Differences in Stress-Strain and Stress-Relaxation Tests Between Several CXL Treatment Conditions, or Between Riboflavin and Virgin Control Conditions

Groups Compared		Stress-Strain *P* Value	Stress-Relaxation *P* Value
0.27% ribo, 1 mo (control)	Virgin (control)	0.0903	0.8018
0.27% ribo, 1 mo (control)	0.5% ribo, 1 mo (control)	0.3456	0.7418
9 mW, 2:50 min, 1 mo	18 mW, 5 min, 1 mo	0.0891	0.8709
9 mW, 2:50 min, 1 mo	9 mW, 10 min, 1 mo	0.3457	0.0749
9 mW, 2:50 min, 1 mo	3 mW, 30 min, 1 mo	0.9780	0.7331
9 mW, 2 min, 1 mo	18 mW, 5 min, 1 mo	0.3457	0.2745
3 mW, 30 min, 1 mo	18 mW, 5 min, 1 mo	0.0903	0.6092
3 mW, 30 min, 1 mo	9 mW, 10 min, 1 mo	0.3457	0.4808
9 mW, 10 min, 1 mo	18 mW, 5 min, 1 mo	0.5407	0.0600
3 mW, 1 min	3 mW, 3 min	0.1700	0.3094

Table 6. Significant Differences From Stress-Strain Analysis, Both Between CXL Treatment Conditions and Between Control Conditions

Groups Compared		Stress-Strain *P* Value	Stress-Relaxation *P* Value
Virgin (control)	0.5% ribo, 1 mo (control)	0.0137	0.1867
9 mW, 10 min	9 mW, 10 min, 1 mo	0.0043	0.1643

R v3.0.2; The R Foundation for Statistical Computing, Vienna, Austria). The statistical comparison between groups was performed globally for the entire parameter set (σ_∞, σ_1, σ_2, τ_1, τ_2). The interested reader can refer to Pinheiro et al.[28] for detailed presentation of these models applied to several biological studies.

For small deformations every material shows a linear stress-strain curve following the Hooke's law. We applied a linear model to describe the relation between stress and strain in a range of 0.05 to 0.5% of strain:

$$F(t) \sim \sigma(t) = \alpha + E \cdot \varepsilon(t) \quad (6)$$

where $F(t)$ is the force, $\sigma(t)$ is the stress, ε the strain, α the intercept, and E the slope. Translated into a mixed linear model thus accounting for the within-subject correlation, the model can be formally written as

$$\begin{aligned} &F_{ijt} = \alpha_{ij} + E_{ij} \cdot \varepsilon_t + \delta_{ijt}, \delta_{ijt} \sim N(0, \lambda^2) \\ &\alpha_{ij} \sim N(\alpha_j, \lambda_a^2), \beta_{ij} \sim N(\beta_{ij}, \lambda_b^2) \end{aligned} \quad (7)$$

Again, the index i is for the subject and j is for the treatment. All random components are independent and normally distributed. The statistical comparison between groups was performed only for parameter E, which represents the elastic modulus.

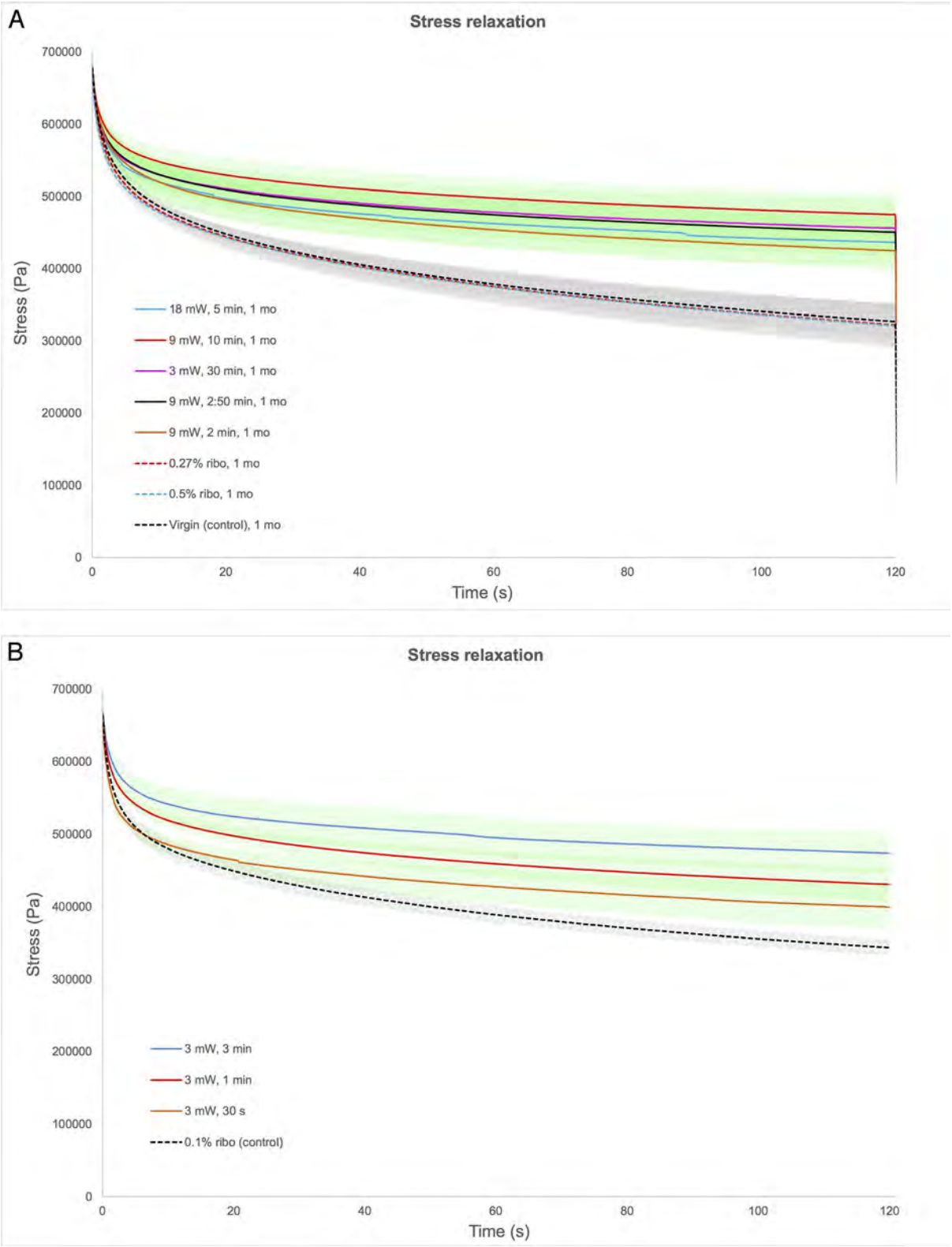

FIGURE 3. Stress-relaxation curves with standard deviation of various treatment (*plain lines*) and control (*dashed lines*) groups. The standard deviations appear in *green* for the treatment groups and in *gray* for the control groups. (**A**) Stress-relaxation curves of the groups of the set 1 showing no superposition between treatment and control group standard deviations. (**B**) Stress-relaxation curves of the groups of the set 2 also showing no superposition between treatment and control groups standard deviations but with a reduced spacing.

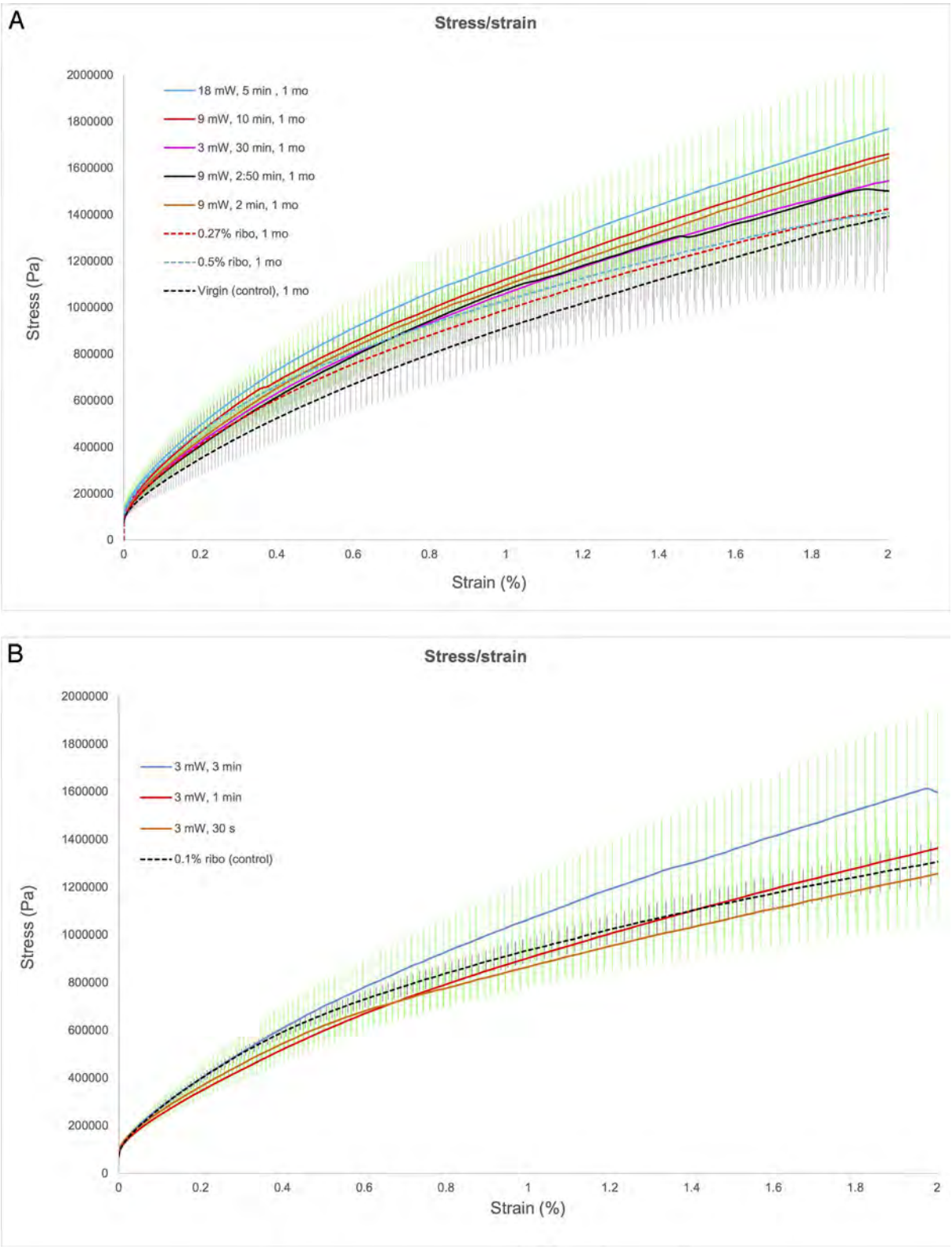

FIGURE 4. Stress-strain curves with standard deviation of various treatment (*plain lines*) and control (*dashed lines*) groups. The standard deviations appear in *green* for the treatment groups and in *gray* for the control groups. (**A**) Stress-strain curves of the groups of the set 1 showing superposition between most of the treatment and control group standard deviations. (**B**) Stress-strain curves of the groups of the set 2 showing superposition between the treatment and control group standard deviations.

Due to the large number of comparisons and the framework complexity, pairwise treatment comparisons were inspected independently using a likelihood ratio test. The *P* values were then adjusted (level of significance = 0.05) using the Benjamini and Hochberg method[29] (Tables 3–6).

Results

Stress-Strain Versus Stress-Relaxation

Both kinds of analysis demonstrated a significantly increased mechanical resistance after CXL. Stress-relaxation tests showed that cross-linked corneas maintained a higher stress (441 ± 40 kPa) than control corneas (337 ± 39 kPa) after 120 seconds of constant strain (Fig. 3). Stress-strain tests showed that cross-linked corneas presented a higher stress at 0.5% strain (778 ± 111 kPa) than control corneas (659 ± 121 kPa), which corresponds to a Young's modulus of 89.7 MPa and 70.9 MPa, respectively (Fig. 4).

Stress-relaxation tests thereby revealed higher significant differences ($P < 0.0001$) between average cross-linked and control conditions than stress-strain tests ($P = 0.008$). Stress-relaxation analysis also proved to be more sensitive in distinguishing minor differences, both between control and CXL treatment conditions, but also between different CXL treatment protocols, while stress-strain analysis was not sensitive enough (Table 4).

Different Irradiances at the Same Fluence

No significant differences were observed for different irradiances at a fluence of 5.4 J/cm^2 in either stress-relaxation or stress-strain tests.

Different Fluences

All corneal cross-linking treatment groups showed a significant difference compared with their corresponding control groups, according to stress relaxation and nonlinear mixed model analysis. Stress-strain tests confirmed this finding in approximately half of the treatment groups (Tables 3, 4).

Stress relaxation could furthermore detect significant differences between certain CXL treatment protocols. Below a fluence of 5.4 J/cm^2, the increase in corneal stiffness after CXL was significantly reduced (Table 4). An unexpected significant difference between control groups was observed in stress-strain testing (Table 6).

Immediate Effect of CXL Versus 1 Month After

The application of the photosensitizer solution affected significantly the biomechanical response on the short term, as riboflavin control conditions were significantly different when compared at 30 minutes and at 1 month after treatment. A higher stress after relaxation remained at 30 minutes than at 1 month after riboflavin treatment (0.5% ribo versus 0.5% ribo 1 month; $P < 0.0001$ for stress-relaxation and $P = 0.0027$ for stress strain; Table 3). In contrast, the effect of CXL was less affected by the short-term effect of riboflavin: Stress-relaxation tests showed no significant differences for a fluence of 5.4 J/cm^2 with an irradiance of 9 mW/cm^2 ($P = 0.1643$). Only stress-strain tests indicated a significant difference ($P = 0.043$), which was close to the level of significance (Table 6).

Discussion

We accurately measured the biomechanical properties of murine corneas at different degrees of in vivo CXL. Two-dimensional extensometry[30] as applied in this study resembles the natural condition in a more realistic way than one-dimensional extensometry, which has been used for the biomechanical analysis of porcine, rabbit, and human corneas.[6,16] We could confirm the finding of a previous study[17] that viscoelastic testing approaches, such as stress-relaxation or creep tests, are more sensitive to measure the effect of CXL.

Although both elastic (stress-strain) and viscoelastic (stress-relaxation) testing showed significant differences between CXL treated and control groups, these differences are distinctly more obvious in the stress-relaxation than in the stress-strain test. This may explain why previous studies[10,31] analyzing the stress-strain of ex vivo porcine corneas required a higher number of samples to obtain significance. A main fact is that for detecting differences between CXL treatment protocols the stress-relaxation test should be preferred.

The stress-strain testing procedure applied in the current study might not be directly comparable with standard stress-strain extensometry. An important difference is that stress was applied in three dimensions instead of uniaxially, which implies that a higher force is required to induce a similar extension.

Given that even the lowest fluence in our study showed a significant increase in stress resistance after relaxation, the minimal necessary fluence for effective CXL in murine corneas is smaller or equal to 0.09 J/cm^2. Even when considering the thinner corneal thickness of mice (1/5), this is lower than expected, when compared with CXL in humans, where the fluence is 60 times higher. We did not observe a decrease in the biomechanical CXL effect when increasing irradiance with constant fluence, as previously reported in ex vivo porcine corneas.[10] This might be explained by a higher oxygen diffusion, and hence higher oxygen availability, in the mouse cornea (100 μm[26]) compared with porcine (877.6 μm[32]) and human (530 μm[27]) corneas. The oxygen dependency of CXL in murine and porcine corneas[33] and other parameters (Kling S, Hammer A, Conti A, Hafezi F, unpublished data, 2015), including keratocyte apoptosis and the overall healing process, are the subject of two parallel studies from our group.

Using a mouse model to study the effect of CXL will create opportunities to investigate the effect of gene modification on the biomechanical changes after CXL, and may help developing new and more efficient treatment protocols.

Acknowledgments

Supported by the Swiss National Science Foundation (OR, AH), and the Gelbert Foundation (DT).

Disclosure: **A. Hammer**, None; **S. Kling**, None; **M.-O. Boldi**, None; **O. Richoz**, None; **D. Tabibian**, None; **J.B. Randleman**, None; **F. Hafezi**, None

References

1. Spoerl E, Huhle M, Seiler T. Induction of cross-links in corneal tissue. *Exp Eye Res*. 1998;66:97–103.
2. Spoerl E, Seiler T. Techniques for stiffening the cornea. *J Refract Surg*. 1999;15:711–713.
3. Hafezi F, Kanellopoulos J, Wiltfang R, Seiler T. Corneal collagen crosslinking with riboflavin and ultraviolet A to treat induced keratectasia after laser in situ keratomileusis. *J Cataract Refract Surg*. 2007;33:2035–2040.
4. Raiskup F, Theuring A, Pillunat LE, Spoerl E. Corneal collagen cross-linking with riboflavin and ultraviolet-A light in progressive keratoconus: ten-year results. *J Cataract Refract Surg*. 2015;41:41–46.
5. Richoz O, Mavrakanas N, Pajic B, Hafezi F. Corneal collagen cross-linking for ectasia after LASIK and photorefractive keratectomy: long-term results. *Ophthalmology*. 2013;120:1354–1359.

6. Wollensak G, Spoerl E, Seiler T. Stress-strain measurements of human and porcine corneas after riboflavin-ultraviolet-A-induced cross-linking. *J Cataract Refract Surg*. 2003;29:1780–17855.
7. Wollensak G, Spoerl E, Wilsch M, Seiler T. Endothelial cell damage after riboflavin-ultraviolet-A treatment in the rabbit. *J Cataract Refract Surg*. 2003;29:1786–1790.
8. Wollensak G, Spoerl E, Seiler T. Riboflavin/ultraviolet-A-induced collagen crosslinking for the treatment of keratoconus. *Am J Ophthalmol*. 2003;135:620–627.
9. Sandvik GF, Thorsrud A, Raen M, Ostern AE, Saethre M, Drolsum L. Does corneal collagen cross-linking reduce the need for keratoplasties in patients with keratoconus? *Cornea*. 2015;34:991–995.
10. Hammer A, Richoz O. Arba Mosquera S, Tabibian D, Hoogewoud F, Hafezi F. Corneal biomechanical properties at different corneal cross-linking (CXL) irradiances. *Invest Ophthalmol Vis Sci*. 2014;55:2881–2884.
11. Richoz O, Hammer A, Tabibian D, Gatzioufas Z, Hafezi F. The biomechanical effect of corneal collagen cross-linking (cxl) with riboflavin and UV-A is oxygen dependent. *Transl Vis Sci Technol*. 2013;2(7):6.
12. Kamaev P, Friedman MD, Sherr E, Muller D. Photochemical kinetics of corneal cross-linking with riboflavin. *Invest Ophthalmol Vis Sci*. 2012;53:2360–2367.
13. Mazzotta C, Traversi C, Caragiuli S, Rechichi M. Pulsed vs continuous light accelerated corneal collagen crosslinking: in vivo qualitative investigation by confocal microscopy and corneal OCT. *Eye (Lond)*. 2014;28:1179–1183.
14. Mazzotta C, Traversi C, Paradiso AL, Latronico ME, Rechichi M. Pulsed light accelerated crosslinking versus continuous light accelerated crosslinking: one-year results. *J Ophthalmol*. 2014;2014:604731.
15. Krueger RR, Herekar S, Spoerl E. First proposed efficacy study of high versus standard irradiance and fractionated riboflavin/ultraviolet a cross-linking with equivalent energy exposure. *Eye Contact Lens*. 2014;40:353–357.
16. Sporl E, Schreiber J, Hellmund K, Seiler T, Knuschke P. Studies on the stabilization of the cornea in rabbits [in German]. *Ophthalmologe*. 2000;97:203–206.
17. Richoz O, Kling S, Zandi S, Hammer A, Spoerl E, Hafezi F. A constant-force technique to measure corneal biomechanical changes after collagen cross-linking. *PLoS One*. 2014;9:e105095.
18. Cespi M, Bonacucina G, Misici-Falzi M, Golzi R, Boltri L, Palmieri GF. Stress relaxation test for the characterization of the viscoelasticity of pellets. *Eur J Pharm Biopharm*. 2007;67:476–484.
19. Li LP, Herzog W, Korhonen RK, Jurvelin JS. The role of viscoelasticity of collagen fibers in articular cartilage: axial tension versus compression. *Med Eng Phys*. 2005;27:51–57.
20. Kling S, Marcos S. Effect of hydration state and storage media on corneal biomechanical response from in vitro inflation tests. *J Refract Surg*. 2013;29:490–497.
21. Synowiec E, Wojcik KA, Izdebska J, Blasiak J, Szaflik J, Szaflik JP. Polymorphisms of the apoptosis-related FAS and FAS ligand genes in keratoconus and Fuchs endothelial corneal dystrophy. *Tohoku J Exp Med*. 2014;234:17–27.
22. Ghosh A, Zhou L, Ghosh A, Shetty R, Beuerman R. Proteomic and gene expression patterns of keratoconus. *Indian J Ophthalmol*. 2013;61:389–391.
23. Li X, Bykhovskaya Y, Tang YG, et al. An association between the calpastatin (CAST) gene and keratoconus. *Cornea*. 2013;32:696–701.
24. Joseph R, Srivastava OP, Pfister RR. Downregulation of beta-actin gene and human antigen R in human keratoconus. *Invest Ophthalmol Vis Sci*. 2012;53:4032–4041.
25. Wang F. UVA/riboflavin-induced apoptosis in mouse cornea. *Ophthalmologica*. 2008;222:369–372.
26. Lively GD, Jiang B, Hedberg-Buenz A, et al. Genetic dependence of central corneal thickness among inbred strains of mice. *Invest Ophthalmol Vis Sci*. 2010;51:160–171.
27. Doughty MJ, Zaman ML. Human corneal thickness and its impact on intraocular pressure measures: a review and meta-analysis approach. *Surv Ophthalmol*. 2000;44:367–408.
28. Pinheiro JC, Bates, DM. *Mixed-Effects Models in S and S-Plus*. New York: Springer; 2000.
29. Benjamini Y, Hochberg Y. Controlling the false discovery rate: a practical and powerful approach to multiple testing. *J R Stat Soc Series B Methodol*. 1995;57:289–300.
30. Kling S, Ginis H, Marcos S. Corneal biomechanical properties from two-dimensional corneal flap extensiometry: application to UV-riboflavin cross-linking. *Invest Ophthalmol Vis Sci*. 2012;53:5010–5015.
31. Wernli J, Schumacher S, Spoerl E, Mrochen M. The efficacy of corneal cross-linking shows a sudden decrease with very high intensity UV light and short treatment time. *Invest Ophthalmol Vis Sci*. 2013;54:1176–1180.
32. Sanchez I, Martin R, Ussa F, Fernandez-Bueno I. The parameters of the porcine eyeball. *Graefes Arch Clin Exp Ophthalmol*. 2011;249:475–482.
33. Kling S, Richoz O, Hammer A, et al. Increased biomechanical efficacy of corneal cross-linking in thin corneas due to higher oxygen availability. *Refract Surg*. In press.

Appendix

Stress

Stress σ was calculated starting from the standard equation:

$$\sigma = \frac{F}{A_{\perp}}$$

where F is the force applied and $A_{\perp}$ is the cross-sectional area orthogonal to the applied force.

For a better understanding, we consider first a standard flap test. Typically one end of the flap in fixed, while at the other end a given force F_{flap} is applied. This means the flap has to resist a net force of $2 \cdot F_{flap}$, but at each end one cross-section of the flap has to withstand F_{flap}. Therefore, the stress in the flap is defined as:

$$\sigma = \frac{F_{flap}}{A_{\perp}}$$

with

$$A_{\perp} = flap_{width} \cdot flap_{thickness}$$

Considering now a flap within an entire cornea in 2D testing (see Fig. A1A, yellow area): Here a given force F is applied at the center of the flap, which is in this case also the net force. The corresponding area that has to withstand this force is $2 \cdot A_{cross}$. Therefore, the stress in a flap with the 2D testing system is defined as

$$\sigma = \frac{F_{flap}}{2 \cdot A_{\perp}}$$

with

$$A_{\perp} = flap_{width} \cdot th$$

Considering now the entire cornea in 2D testing: As before, the applied force F_{flap} corresponds to the net force. The cross-sectional area resisting this force is here

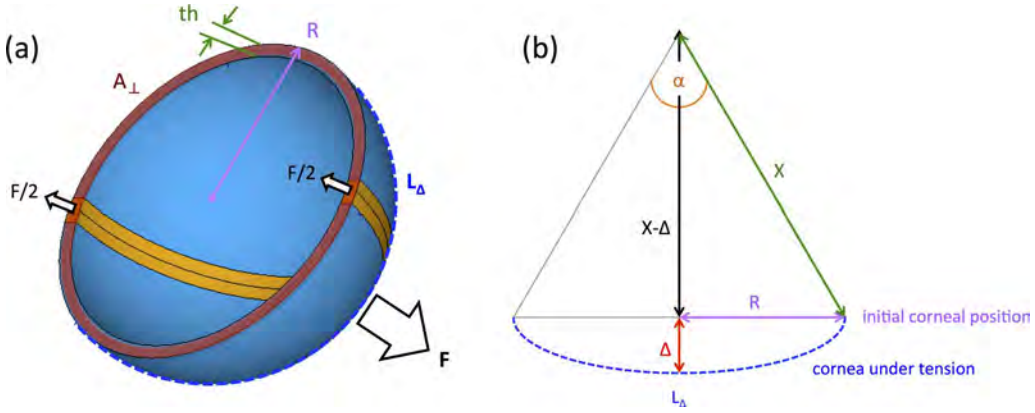

Figure A1. Parameters used for the calculation of (**A**) stress and (**B**) strain.

$$A_{\perp} = 2\pi \cdot R \cdot th$$

and, hence, corneal stress is defined as

$$\sigma = \frac{F}{2\pi \cdot R \cdot th}$$

Strain

For the calculation of corneal strain we considered the sketch shown in Figure A1B.

The assumption was made that at each indentation Δ the cornea adapts the shape of an ideal sphere with radius X. The arc-length L_{Δ} is then defined by

$$L_{\Delta} = \alpha \cdot X$$

where α is the angle of the circular sector. Applying trigonometry, α and X can be expressed as a function of indentation Δ and radius of the holder R:

$$\alpha = 2 \cdot \sin^{-1}\left(\frac{R}{X}\right)$$

$$X = \frac{\Delta^2 + R^2}{2\Delta}$$

Strain is defined as the relative change in length of the tested cross-section and can hence be calculated by

$$\varepsilon_{tensile} = \frac{L_{\Delta} - 2R}{2R} = \frac{\Delta^2 + R^2}{2\Delta R} \cdot \sin^{-1}\left(\frac{2\Delta R}{\Delta^2 + R^2}\right) - 1$$